arXiv:0903.4306v1 [cond-mat.mtrl-sci] 25 Mar 2009

Adsorption of benzene, phenol, propane and carbonic acid molecules on oxidized Al(111) and α-Al_2O_3(0001) surfaces: A first-principles study

Janne Blomqvist and Petri Salo

Department of Applied Physics, Helsinki University of Technology, P.O. Box 1100,
FI-02015 TKK, Finland

Abstract. We present the results of *ab initio* calculations describing the adsorption of certain small organic molecules on clean and oxidized Al(111) surfaces as well as on the α-Al_2O_3(0001) surface. Our results show that adsorption of benzene on the clean and oxidized Al(111) surfaces is generally weak, the adsorption energy being at most around -0.5 eV per benzene molecule, and the molecule adsorbed at a considerable distance from the surfaces. The adsorption energy varies weakly at the different adsorption sites and as a function of the oxygen coverage. For the alumina surface, we find no benzene adsorption at all. We have also calculated a phenol molecule on the aluminium and alumina surfaces, since it is similar to the benzene molecule. The results show a weak adsorption for phenol on the alumina surface and no adsorption on the aluminium or oxidized aluminium surfaces at all. For the propane molecule there is no adsorption on either the oxidized aluminium or the alumina surface, whereas the carbonic acid molecule binds strongly to the alumina but not to the aluminium surface.

Aluminium, Oxygen, Aromatics, Carbonic acid, Propane, Density functional calculations, Adsorption

1. Introduction

Hybrid materials, where multiple substances are combined, belong to an interesting new class of materials. These materials can be optimized for specific applications, emphasizing appearance, strength or some other property [1]. To understand these materials we must understand the interface between the various substances.

Particularly interesting materials from a practical as well as a scientific perspective are the materials that combine a metal and polymer. Studying the interface between these substances at the microscopic scale is of a great importance. Thus, studying the interaction between the metal surface and the molecules in the polymer chains is important. There are also multiple adhesion mechanisms that need to be understood, such as mechanical gripping, and multiple phenomena affecting the strength of the interface, such as the surface roughness and wetting. In this work, however, we have focused on the microscopic scale quantum mechanical binding between the aluminium surface and organic compounds common in polymers using first-principles calculations.

Real aluminium surfaces oxidize very quickly when in contact with the atmosphere. To investigate how the oxygen coverage affects adsorption, we have used density functional theory to calculate the adsorption energy at different oxygen coverages. Aluminium is also often electrolyzed to increase corrosion resistance. During the electrolyzing process, a layer of alumina is formed on the aluminium surface. Thus, we have also investigated the adsorption of the molecules on the α-alumina (0001) surface. The (0001) surface of alumina was chosen because it has been extensively studied in the past, both experimentally and computationally.

Previously there has been relatively little work on the systems of organic molecules on aluminium surface, either computational or experimental. Duschek et al. [2] studied benzene on clean Al(111) both computationally and experimentally, and Chakarova-Käck et al. [3] studied phenol on α-Al_2O_3(0001) using density functional theory calculations with van-der-Waals corrections. Su et al. [4] studied carbonic acid anions in solution adsorbing on an amorphous alumina surface, showing that carbonic acid adsorbs on top of the Al atom in the alumina substrate. Similarly, Alliot et al. [5] studied carbonic acid anions on an α-Al_2O_3 surface, showing the presence of adsorption. Johnston et al. [6] studied the adsorption of the bisphenol-A-polycarbonate (BPA-PC) on the Si(001) surface component molecules using density functional theory calculations.

In this paper we have calculated the adsorption of benzene, phenol, carbonic acid and propane on the close packed Al(111) and α-Al_2O_3(0001) surfaces. With these molecules one could build up a BPA-PC molecule, which is an important polycarbonate plastic. The benzene molecule has been placed at the fcc, hcp, bridge and top sites, with different amounts of oxygen on the Al(111) surface. The oxygen molecule is either at the fcc or hcp hollow site, or there are two nearest neighboring oxygens at adjacent fcc and hcp sites. Finally, we have also calculated the case where the Al(111) surface is covered by one monolayer (ML) oxygen at the fcc sites. For the other components and the α-Al_2O_3(0001) surface only a few configurations have been calculated, with the component molecule on the top of an Al and O atom or at the hollow sites.

The rest of the paper is organized as follows. First, in Section 2 we give a brief outline of the computational techniques we have used, in Sections 3.1 and 3.2 we present our results for the Al(111) and α-Al_2O_3(0001) surfaces, respectively, and finally we discuss our results and give some concluding remarks in Section 4.

2. Methods

We have used the *Vienna Ab Initio Simulation Package* (VASP) [7, 8, 9], a program for calculating the energy ground state using a plane wave basis set. The many-body effects have been taken into account with the revised version [10] of the Perdew-Burke-Ernzerhof (PBE) [11] form of the generalized gradient approximation, which is known to produce better molecular adsorption energies compared to vanilla PBE, however, at the expense of a bigger error in the lattice constant compared to full potential calculations. For the potentials we have used the projector augmented wave method [12, 13] with a plane wave cutoff energy of 400 eV.

For the Al(111) calculations, a supercell with 4x4x4 Al atoms has been used, while for the alumina calculations we have used a larger Al-terminated supercell with 48 Al and 72 O atoms in 12 Al and 6 O layers, forming a 2x2 hexagonal surface supercell. The thickness of the slab for the Al case was 7.9 Å, while the alumina slab was thicker being 12.2 Å, in order to take into account the large surface relaxations in the Al-terminated alumina surface [14]. For the Al case, there was 16.5 Å vacuum between the periodic slabs, while for alumina the corresponding value was 14.0 Å.

The Brillouin zone was sampled using the Monkhorst-Pack scheme [15, 16], and the number of k points in the irreducible part of the Brillouin zone was 15 (5x6x1 mesh) for the oxygen covered Al(111) surface and 4 k-points (2x2x1 Γ-centered mesh) for the α-Al_2O_3(0001) surface. In the case of the Al(111) surface the k-point grid was nonuniform in the surface plane since the surface cell used was rectangular, and thus the length of the lattice vectors in the plane were not equal. Hence we tested different combinations of k-point grids before choosing the 5x6x1 grid. To make the convergence towards the electronic ground state faster the Fermi level was smeared using the method of Ref. [17] with a value of 0.2 eV for the metal surface, and for the alumina surface we used Gaussian smearing with a smearing parameter of 0.4 eV. Test calculations were made with spin polarization enabled; no spin polarization was seen and thus the rest of the calculations were made without spin polarization to reduce the computational burden. In order to account for potential charge inbalance on the surfaces in the cell, a dipole correction was applied in the direction normal to the surface.

Atomic coordinates were relaxed until forces were less than 0.02 eV/Å, and k-point grids were chosen to make the error in total energy less than 0.05 eV. The same procedure was followed during the adsorption energy calculations, that is, the molecules were placed in approximate starting positions and allowed to relax freely until forces were less than 0.02 eV/Å.

For the analysis of the local density-of-states (LDOS), one needs to compare the LDOS's of different systems with each other. Thus, the energy scales have to be comparable. For the reference system for each plot, typically the surface slab with a molecule adsorbed, the calculated Fermi energy E_F was subtracted,

$$E' = E - E_F \,,$$

where E is the tabulated energy. For the calculations used for comparing with the reference system, such as a molecule in vacuum, the energy was shifted as

$$E' = E - E_F - (\phi - \phi_{ref}) = E - E_{F,ref} - (E_{vac} - E_{vac,ref}) \,,$$

where $\phi = E_{vac} - E_F$ is the work function of the system, ϕ_{ref} is the work function of the reference system, E_{vac} is the maximum z-averaged vacuum potential in the supercell of the system, and $E_{vac,ref}$ is the maximum z-averaged vacuum potential for the reference system.

3. Results and discussion

In this section we show our results for the molecules on the Al(111) and α-Al_2O_3(0001) surface. The molecules with their chemical compositions are benzene (C_6H_6), phenol (C_6H_5OH), carbonic acid (H_2CO_3), and propane (C_3H_8). We define the coverage of a molecule on the surface as the number of molecules per atoms in the surface layer. For each system we calculate the electronic and geometric structure and the total energy. We define the adsorption energy as

$$E_{ads} = E_{tot} - E_{slab} - E_{mol} \,,$$

where E_{tot} is the total energy of the system with the molecule or atom adsorbed on the surface, and E_{slab} is the total energy of the empty surface slab. The third term, E_{mol} is the total energy of the adsorbed molecule or atom in vacuum calculated using the same cell geometry, k-point grid and other calculation parameters such as smearing, as with the slab calculations. In the case of the calculations on the oxidized surface, E_{slab} is the total energy of the oxidized surface slab.

3.1. Al(111) surface

With the parameters described in the preceding section, the equilibrium lattice constant for bulk fcc aluminium has been calculated to be 4.055 Å, compared to the experimental result of 4.0496 Å [18]. For comparison, with Perdew-Wang 91 [19] and the regular PBE gradient approximations the lattice constants are found to be 4.05 and 4.04 Å, respectively [20], and using the PBE approximation 4.052 Å [2].

For the Al(111) surface with an oxygen coverage, the adsorption energy per oxygen atom has been calculated, and the results can be seen in Table 1. As expected, the

Table 1. Adsorption energy for O on Al(111) per O atom at different coverages. Individual atoms at the fcc and hcp sites, two oxygen atoms at nearest neighbor (nn) fcc and hcp sites, and 1 ML of oxygen atoms at the fcc sites. The energies are with respect to atomic oxygen in vacuum; with respect to an half of the energy of the O_2 molecule in vacuum, 3.19 eV should be added to the tabulated values.

	Ads. energy (eV)
fcc/0.0625 ML	−7.27
hcp/0.0625 ML	−6.94
nn/0.125 ML	−7.00
fcc/1 ML	−7.71

Table 2. Adsorption energy (eV) for benzene at different sites (with and without $\frac{\pi}{6}$ rotation around the axis perpendicular to the surface) on Al(111) with the benzene coverage of 0.063 ML and with different oxygen coverages.

O$\diagdown C_6H_6$	fcc	fcc $\frac{\pi}{6}$	hcp	hcp $\frac{\pi}{6}$	bridge	bridge $\frac{\pi}{6}$	top	top $\frac{\pi}{6}$
clean	0.12	0.12	0.08	0.12	0.12	0.12	0.21	0.21
fcc	0.16	0.16	0.25	0.25	0.15	0.16	0.14	0.15
hcp	0.19	0.20	0.33	0.32	0.20	0.20	0.20	0.19
nn	−0.52	−0.51	0.13	0.14	−0.52	−0.52	−0.52	−0.51
1 ML	0.17	0.17	0.17	0.18	0.17	0.18	0.17	0.18

highest adsorption energy for a single O atom was found at the fcc site. When the entire surface was covered with 1 ML oxygen at the fcc sites, the adsorption energy per oxygen atom was 0.44 eV lower than for an isolated oxygen atom, indicating that the aluminium surface oxidizes very easily. For the fcc and hcp sites, the results are comparable to other calculations [21]. More detailed calculations describing the behavior of oxygen on Al(111) can be found in Refs. [21, 22, 23].

3.1.1. Benzene In Table 2 one can see the adsorption energy of benzene as it adsorbs on the Al(111) surface with different O coverages. One can see that with the exception of the configuration with nearest neighbor oxygens at the fcc and hcp sites, where the adsorption energy is about −0.5 eV, there is very weak or no adsorption at all. In Fig. 1, one can see an example of a configuration, with the benzene molecule at the fcc site.

The work functions for the surfaces were also calculated. In all the cases except for the one with 1 ML oxygen, the work function was between 4.0 and 4.1 eV. For the 1 ML case, it was between 4.5-5.0 eV depending on the location of the benzene molecule.

In all the cases, the equilibrium distance above the surface for the benzene molecule was about 4.0 Å, also for the cases of the nearest neighbor O on Al(111) where the adsorption of benzene was observed. By comparing charge density differences between the benzene molecule and Al(111) slab separately and when the molecule was on the surface, we saw that there was no charge transfer between the benzene molecule and the surface. To analyze further the situation we have plotted the LDOS with specific

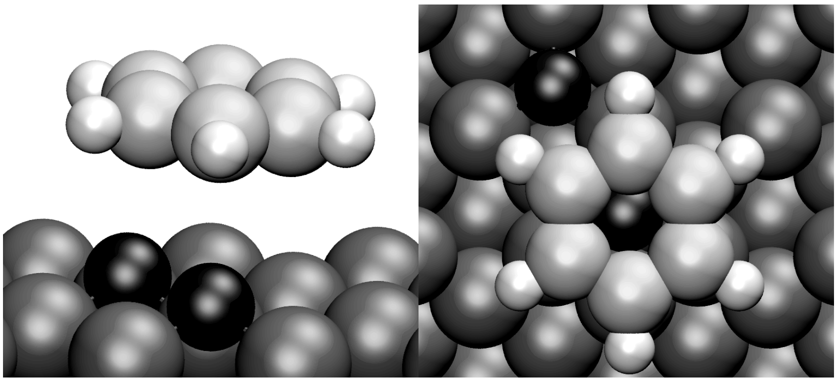

Figure 1. A side (left) and top (right) view of the benzene molecule on top of the fcc site on the Al(111) surface, without the $\frac{\pi}{6}$ rotation and with nearest neighbor oxygens on the surface. Hydrogen atoms are seen as small light gray spheres, carbon as large light gray spheres, oxygen as large black spheres, and aluminium as large dark gray spheres.

angular projections for different atoms in the system. In Fig. 2, for Al atoms in the surface layer on the Al(111) surface with nearest neighbor oxygens on the surface, one can see that there is practically no difference in the LDOS of Al for the cases where the Al atom is below the benzene or on an empty surface. However, in Fig. 3 one can see that the presence of the benzene molecule causes a change in the p-LDOS of the oxygen atoms on the surface. There is almost no difference whether the oxygen atom is directly below the center of the benzene molecule or slightly offset. Thus, the adsorption of benzene has to be due to the mutual binding to both of the oxygen atoms on the surface (see also Table 2).

We can compare our results with other experimental and computational results [2]. In contrast to the value reported for the equivalent clean surface configuration in Ref. [2], -0.351 eV, we found no adsorption on the clean surface, though it should be mentioned that we used a different potential functional. Despite our efforts, we have been unable to reproduce the adsorption energy reported there, even if we used the same potential and with a denser k-point grid than normal (11x11x1). However, the other observations in Ref. [2], that i.e. the density of states are not changed substantially and the distance of C_6H_6 from the surface is quite large, as well as the photoemission and thermal desorption spectras, indicate that the binding of C_6H_6 to the Al(111) surface is rather weak, which is in line with our results.

We have also calculated the C_6H_6 coverage dependence on the adsorption energy. We only checked the system of benzene at the fcc site with the nearest neighbor oxygen on the Al(111) surface. By putting two benzene molecules in the original 4x4 supercell, the adsorption energy for the coverage of 0.125 ML was found to be -0.51 eV which does not differ too much from the value of -0.52 eV for the 0.063 ML case. Thus, we saw no coverage dependency in the adsorption energy.

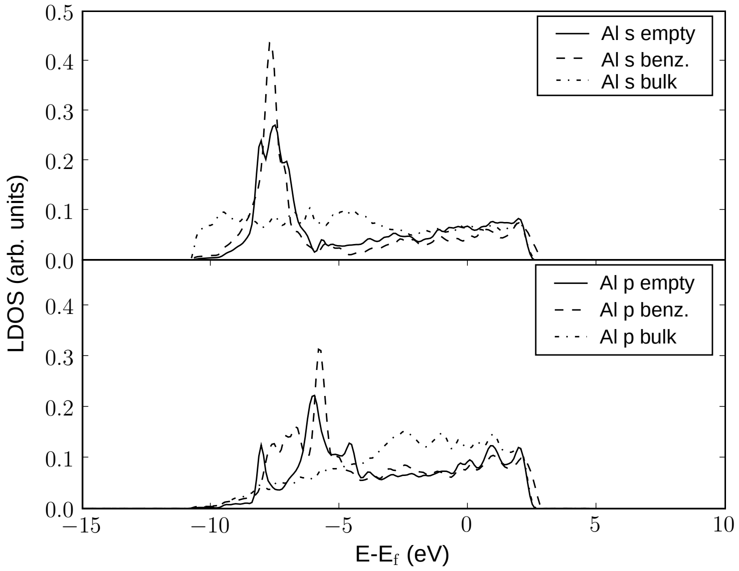

Figure 2. LDOS for the Al atoms in the surface layer of the Al(111) surface with nearest neighbor oxygens present, without (solid lines) and with (dashed lines) a benzene molecule (fcc $\frac{\pi}{6}$ site). For comparison the LDOS for an atom in bulk Al (chain line) can also be seen. Coverage of C_6H_6 is 0.063 ML.

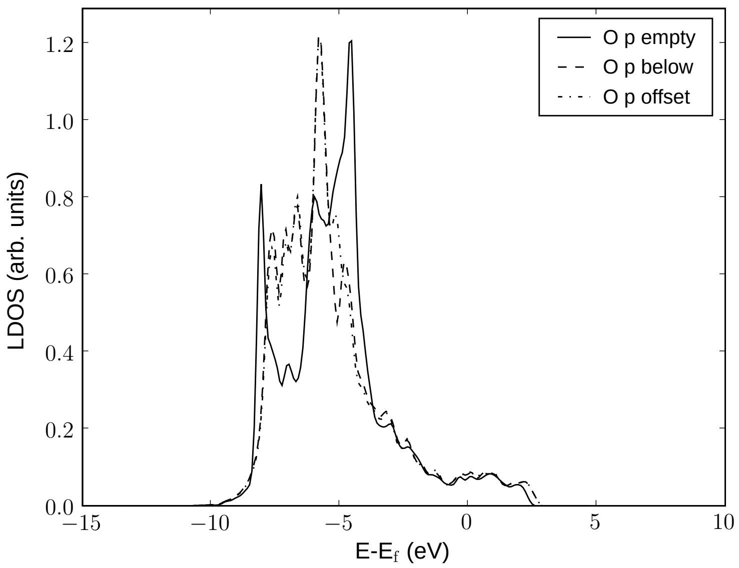

Figure 3. p-LDOS for the nearest neighbor oxygens on the Al(111) surface, without (solid line) and with (dashed and chain lines) a benzene molecule at the fcc $\frac{\pi}{6}$ site. When the benzene molecule is present, the oxygen is either directly below the center of the benzene molecule (dashed line), or offset from the center by about 2.4 Å in the next hollow site (chain line). Coverage of C_6H_6 is 0.063 ML.

Table 3. Adsorption energies of phenol on the clean and oxidized Al(111) surface. In all cases the oxygen in the phenol molecule is at the fcc hollow site on the (111) surface.

	clean	fcc	hcp	nn	1 ML
Ads. energy (eV)	0.07	0.08	0.07	0.02	0.00

3.1.2. Phenol As the adsorption energy of the benzene molecule was not particularly dependent on the adsorption site, we decided not to test the phenol molecule (C_6H_5OH) as exhaustively as the benzene molecule. In all cases the phenol molecule was placed over the surface such that the oxygen atom in the phenol was on the top of the fcc site. Thus, as we previously found out that benzene does not adsorb to the clean surface, and when it shows some adsorption there must be some oxygen on the surface, the working hypothesis is that the phenol molecule would bind to the surface via the oxygen atom, with the hydrogen atom in the hydroxyl group potentially dissociating. The results can be seen in Table 3. In general, the results are comparable to those of benzene, i.e. there is no adsorption at all. The main difference is that while for the case of benzene, the nearest neighbor configuration (where there were two oxygen atoms in neighboring fcc and hcp sites) exhibited some adsorption, for phenol there is no adsorption in that case either.

3.1.3. Propane For the case of propane (C_3H_8), we tested only the fcc site on the clean Al(111) surface. The only part of the propane molecule that can come in contact with the surface, is one of the two CH_3 groups at the ends. Thus, we tested the case when the propane molecule is sitting upright on the surface, with only one of the CH_3 groups touching the surface, as it can be seen in Fig. 4. However, we found no adsorption, rather the propane molecule moved away from the surface during the relaxation. This was the expected result, as the propane molecule has no dangling bonds available to form new bonds to the surface in the CH_3 endgroup.

3.1.4. Carbonic acid In Fig. 5 one can see a carbonic acid molecule (H_2CO_3) at the fcc site on the clean Al(111) surface. Due to the hydrogen atoms, only the oxygen atom with the double bond to the carbon atom is free to react with the surface. Thus, we only studied the case when the said oxygen was closest to the fcc site, and no other orientations of the molecule. During the relaxation, the molecule moved away from the surface, while simultaneously tilting until lying almost flat in the final configuration. In the final configuration the molecule was at a distance of 3.4 Å, and the adsorption energy was 0.00 eV, i.e. no adsorption.

3.2. α-Al_2O_3(0001) surface

A side view of the alumina surface and a schematic top view with adsorption sites can be seen in Fig. 6.

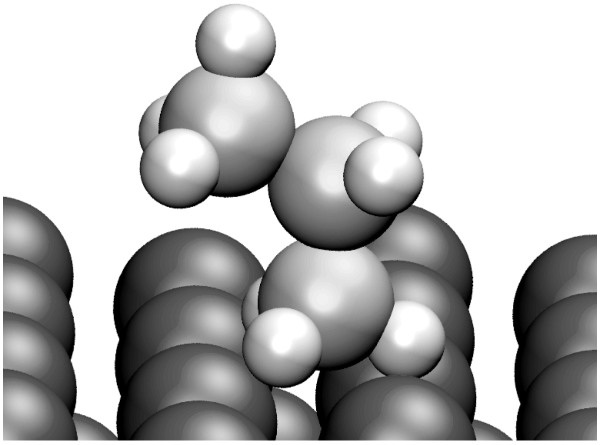

Figure 4. A propane molecule on top of the clean Al(111) surface. Hydrogen atoms are seen as small light gray spheres, carbon as large light gray spheres, and aluminium as large dark gray spheres.

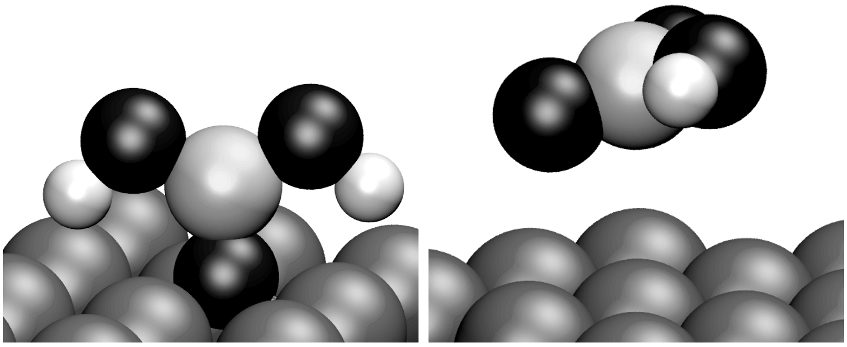

Figure 5. A carbonic acid molecule on top of the clean Al(111) surface. Start (left) and final configuration (right). Hydrogen atoms are seen as small light gray spheres, carbon as large light gray spheres, oxygen as large black spheres, and aluminium as large dark gray spheres.

3.2.1. Benzene For the alumina surface, the adsorption energies of benzene are also very weak. A benzene molecule adsorbed at the top site over an O atom had an adsorption energy of $-0.09/-0.05$ (without/with the $\frac{\pi}{6}$ rotation) eV, while on the top site over an Al atom the adsorption energy was 0.02/0.02 eV. For the hollow size above an Al atom, the adsorption energy was 0.01/0.02 eV, that is, no adsorption. For the O top case, where the benzene molecule did not move away into the vacuum, the molecule preferred to be in a tilted position, with an angle of 12.8°. This configuration can be seen in Fig. 7. When compared to the case in which the benzene molecule binds weakly to the Al(111) surface with two nearest neighbor oxygen atoms on it, we can conclude that increasing further the number of oxygen atoms in the surface layer decreases the binding character of C_6H_6 on Al(111) surfaces.

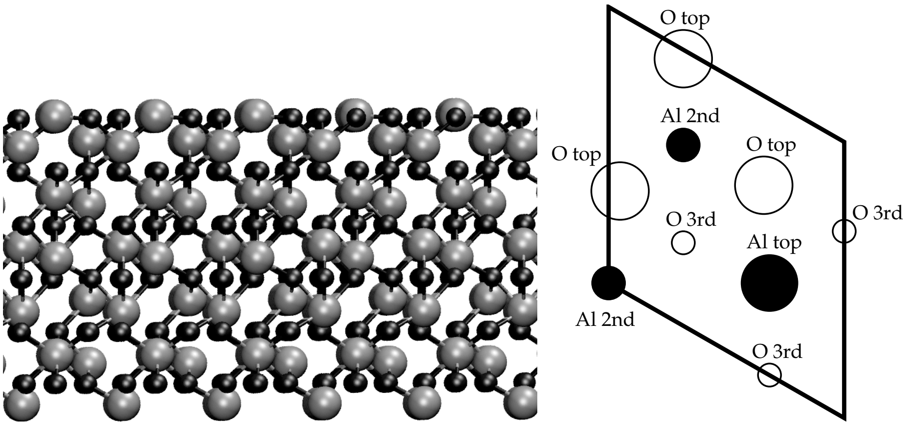

Figure 6. General view (left) and surface atoms (right) on the Al-terminated α-$Al_2O_3(0001)$ surface. On the left panel, Al atoms are large light grey spheres, O atoms small dark grey spheres, and the radius of the spheres is proportional to the Wigner-Seitz radii of the atoms. On the right, Al atoms are filled circles, and O atoms empty circles. Due to the alumina surface relaxation the uppermost Al and O layer are almost at the same height, then 2nd layer with Al atoms is seen with smaller circles, and finally the 3rd layer O atoms are seen with still smaller circles. The primitive surface supercell box can also be seen, whereas the calculations used a 2x2 surface supercell.

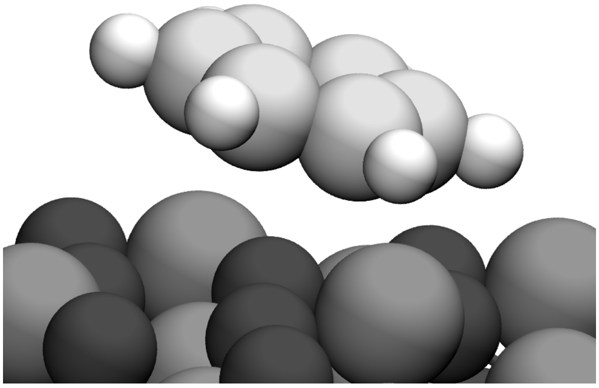

Figure 7. A benzene molecule on top of an O atom on α-$Al_2O_3(0001)$. Hydrogen atoms are seen as small light gray spheres, carbon as large light gray spheres, oxygen as large black spheres, and aluminium as large dark gray spheres.

3.2.2. Phenol For phenol, we did only a test calculation to check that our adsorption geometry and energy were in the same ballpark as those reported in Ref. [3], to which we refer the reader interested in more detailed calculations for phenol on Al-terminated α-$Al_2O_3(0001)$. For the most promising case, labeled (ii) in Ref. [3], we found an adsorption energy of -0.66 eV vs. -1.00 eV in Ref. [3]. This difference is probably due to different potentials and parameters used in our simulations. However, the adsorption geometry was essentially identical, with the phenol molecule adsorbing at an angle of 42.4° vs. 44.7° in Ref. [3], and the OH bond in the phenol molecule bent in a similar way.

3.2.3. Propane For this system two configurations were tested, with the CH_3 end group of the propane molecule at the Al hollow site and at the O hollow site on the α-Al_2O_3(0001) surface. The configuration of the propane molecule on the surface was the same as for the Al(111) surface, which can be seen in Fig. 4. In both these cases the propane molecule moved away from the surface without adsorbing, as also happened with the case of the Al(111) surface.

3.2.4. Carbonic acid Contrary to the case of carbonic acid on the Al(111) surface, we found a significant change in total energy for the carbonic acid molecule on α-Al_2O_3(0001). Allowing the carbonic acid molecule to freely relax on the surface, resulted in the molecule moving to the Al-top site, with the non-hydrogenated oxygen lying closest to the surface Al-top atom at a distance of 1.81 Å. Also, one of the passivating hydrogens detached from the molecule and adsorbed at the surface O-top site. This configuration, with the reduction in total energy of −1.91 eV, can be seen in Fig. 8. Separating the contributions from the carbonic acid molecule and the hydrogen atom reveals that much of this energy is due to the rearrangement of the bonding of the hydrogen atom. The bond dissociation energy for the hydrogen atom from the carbonic acid molecule in vacuum was found to be −5.74 eV, whereas the adsorption of a hydrogen atom at the O top site on the α-Al_2O_3(0001) surface was −4.14 eV. Hence there is a change in the bonding energy of the hydrogen atom of +1.60 eV, and thus in the above system the contribution of the carbonic acid molecule to the total adsorption energy of −1.91 eV was −3.50 eV. Experimental results show qualitateively similar behaviour [5, 4].

Comparing the LDOS for the oxygen atom with the double bond in the carbonic acid molecule when the molecule is adsorbed at the Al top site on the α-Al_2O_3(0001) surface and in vacuum, we can see what happens when the molecule adsorbs (see Fig. 9). One can see that when the molecule is present on the surface, the LDOS is in general smeared out, and especially for the p-LDOS there is a shift from the peaks at −5 and−8 eV towards multiple smeared out peaks between −10 and 0 eV. Also the s peak around −8 eV splits into a band between −10 and −2 eV.

Comparing the LDOS's for the oxygen with the LDOS's for the carbon atom in the carbonic acid molecule (see Figs. 9 and 10), one sees similar kind of broadening of the molecular orbital states of C as for O. On the other hand, the LDOS's of the aluminium atom on the surface closest to the carbonic acid molecule also change (see Fig. 11). The s states at +5 eV shift to +8 eV and the peak at −6 eV below the Fermi level shifts to −8 eV. For the p states, the peak at +5 eV vanishes, while the one at +7 eV shits up to +9 eV. There are also smaller changes in the band between −10 and 0 eV, showing a shift of the energy bands to lower energies. These changes match those of the oxygen atom in Fig. 9. Thus, the binding character of the alumina surface increases which can also be seen in the adsorption energy of the carbonic acid molecule on the surface.

The change in the binding of the H atom as it detaches from the carbonic acid molecule and attaches to the alumina surface can be seen in Fig. 12. One can clearly

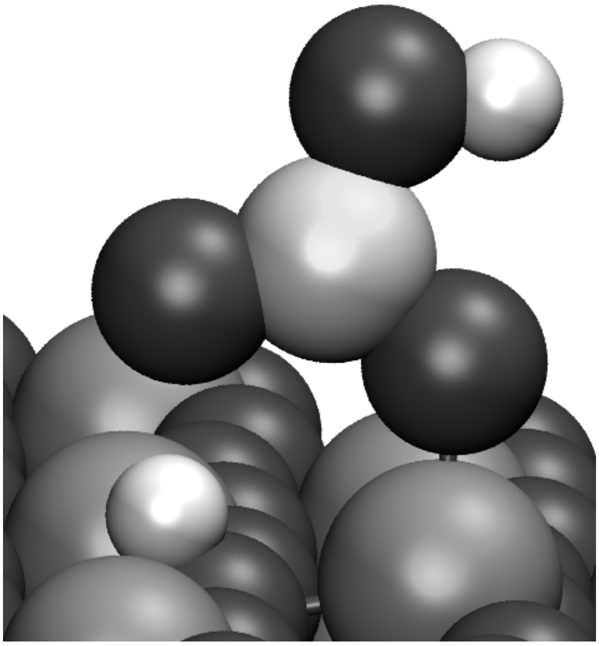

Figure 8. A carbonic acid molecule adsorbed on the α-Al_2O_3(0001) surface. Hydrogen atoms are seen as small light gray spheres, carbon as large light gray spheres, oxygen as large black spheres, and aluminium as large dark gray spheres.

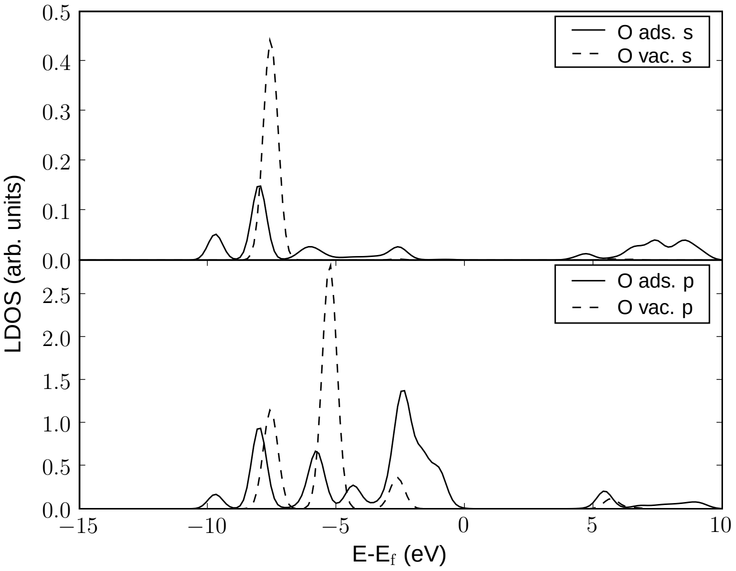

Figure 9. LDOS of the oxygen atom of the carbonic acid molecule bound with a double bond (no H passivation in vacuum) to the carbon atom. In vacuum (dashed lines) and adsorbed at the Al-top site on the Al_2O_3(0001) surface (solid lines). Both s-LDOS (upper panel) and p-LDOS (lower panel) are shown.

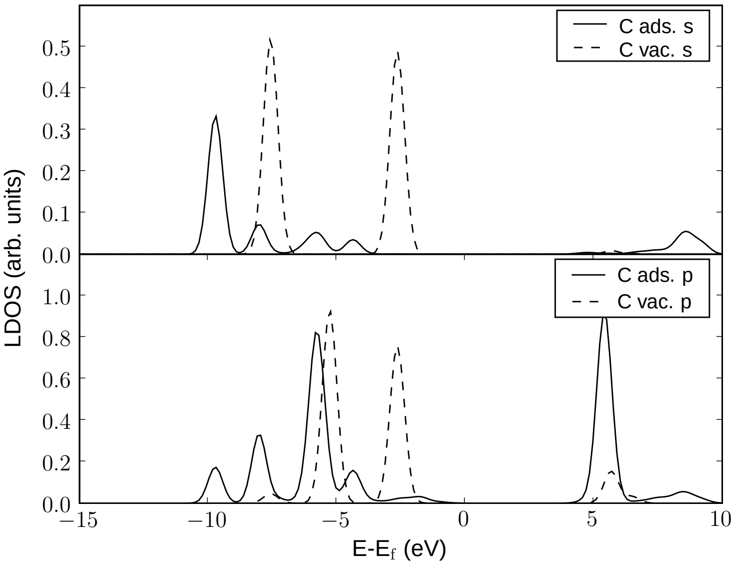

Figure 10. s-LDOS (upper panel) and p-LDOS (lower panel) of the carbon atom in the carbonic acid molecule in vacuum (dashed lines) and adsorbed at the Al-top site on the $Al_2O_3(0001)$ surface (solid lines).

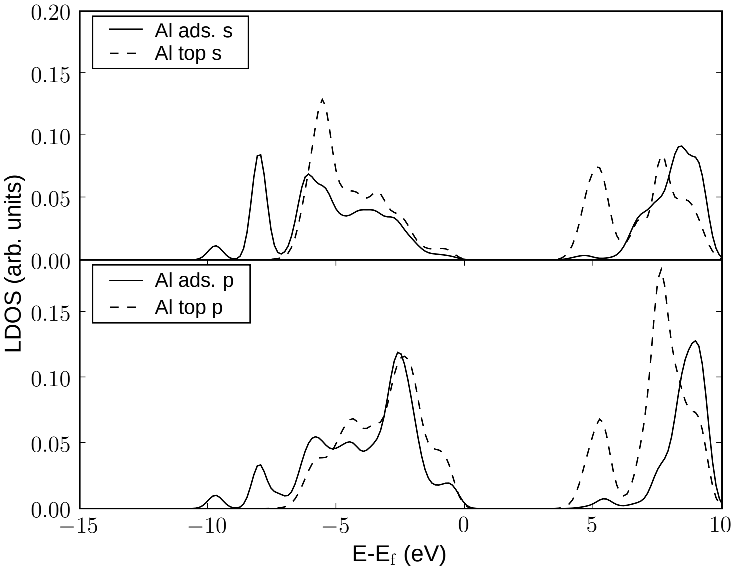

Figure 11. s-LDOS (upper panel) and p-LDOS (lower panel) of the aluminium atom in the surface layer of the $Al_2O_3(0001)$ surface without (dashed lines) and with (solid lines) the carbonic acid molecule close to the Al atom.

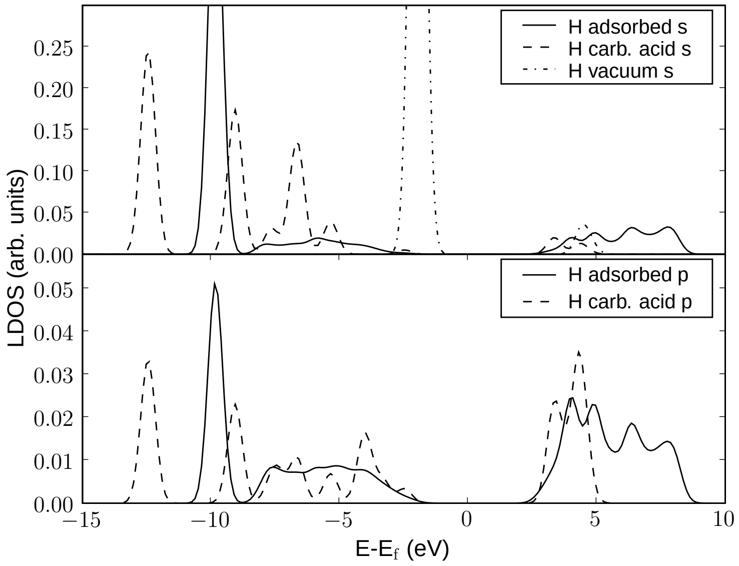

Figure 12. s- and p-LDOS of the H atom at the O-top site on the alumina surface (solid lines), attached to the carbonic acid molecule (dashed lines), and in vacuum (chain line).

see how the atomic energy levels split up and hybridize with the molecular orbitals and the surface band structure, respectively.

In Fig. 13 one can see the p-LDOS of the oxygen atoms in the surface layer and in the second uppermost layer in the surface compared to corresponding oxygen atoms far away from the carbonic acid adsorption site. For the uppermost layer, there is a small change in the peak at −1 eV, except for the oxygen atom to which the detached hydrogen atom has bound. In that case the peak at −1eV has disappeared, and instead there is a new peak at −10 eV, along with a wide band between −8 and −2 eV which matches the hybridized s and p states of the H atom in Fig. 12. For the second layer oxygen, there is a similar shift as for the uppermost layer oxygens, but of a smaller magnitude.

Finally, by investigating how the charge density has changed due to the adsorption (Fig. 14), one can see that the adsorption process causes a large change of charge between the hydrogen atom on the surface and the closest surface oxygen, as well as the change of charge between the oxygen closest to the surface in the carbonic acid molecule and the surface Al atom it is bonded to. This, like the LDOS analysis above, suggests covalent binding between both the carbonic acid molecule and the surface, and between the detached hydrogen atom and the surface. One can also see that the adsorption causes changes in the charge distribution up to three oxygen layers down into the substrate, when charge moves upwards to compensate for the charge that has moved to the adsorption location.

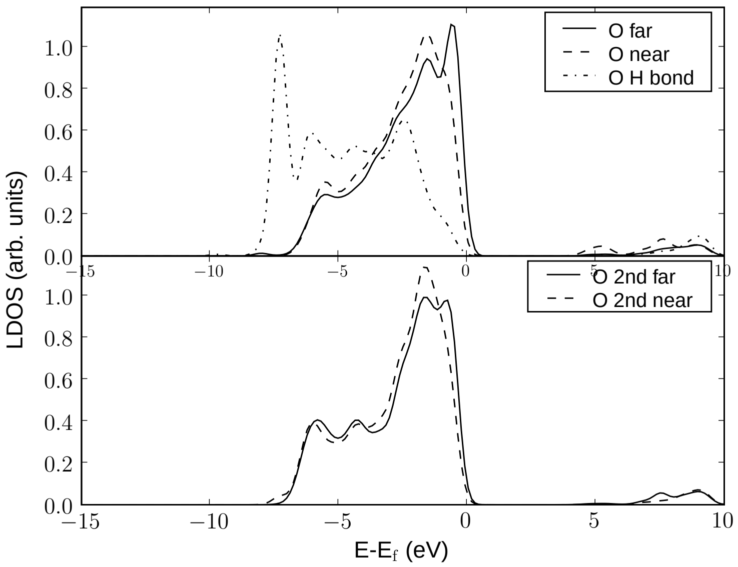

Figure 13. p-LDOS of the oxygen atoms in the uppermost (upper panel) and second uppermost (bottom panel) oxygen layers in the $Al_2O_3(0001)$ surface with an adsorbed carbonic acid molecule. In the upper panel, 'far' refers to an oxygen atom far away from the adsorbed carbonic acid molecule, 'near' refers to an oxygen atom which is the nearest neighbor of the Al atom to which the carbonic acid molecule has bound. Finally, 'H bond' refers to the oxygen atom which the detached hydrogen atom was bound to. In the bottom panel, '2nd' refers to an oxygen atom in the second uppermost oxygen layer far away from the carbonic acid molecule, and '2nd near' refers to an oxygen atom which is the nearest neighbor of the Al atom to which the carbonic acid molecule has bound.

4. Conclusions

We have shown the results for the adsorption of a few specific small organic molecules on the oxidized Al(111) and α-$Al_2O_3(0001)$ surfaces. In general, the adsorption is quite weak, like for benzene on oxidized aluminium and phenol on α-alumina surfaces, and the adsorption distance is significant. The major exception is the carbonic acid molecule which binds strongly to the alumina surface. In general, as opposed to most transition metals, surface chemistry on the aluminium surface is dominated by the high affinity of oxygen to the surface [24], and thus we expected that the adsorption for phenol on alumina would be much stronger than for the benzene molecule. Indeed this was exactly what we saw for carbonic acid, and to a lesser extent phenol on alumina vs. benzene on alumina.

In the future we plan to test a subset of these results while using an exchange-correlation functional taking into account van der Waals (vdW) interactions [25, 26]. In Ref. [3] it was found that for phenol on Al-terminated α-$Al_2O_3(0001)$, taking vdW into account will enhance adsorption by about 0.2 eV. Also, our choice of the RPBE functional, while producing more accurate covalent molecular adsorption energies, does

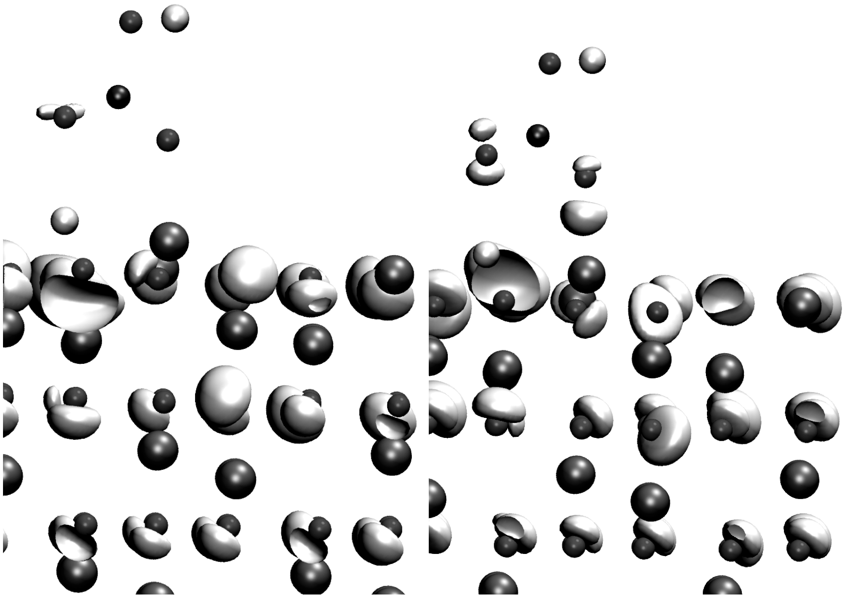

Figure 14. Charge density difference for carbonic acid adsorbed on the alumina surface. On the left, -0.2 Å^{-3} isosurface, and on the right $+0.2$ Å^{-3} isosurface. Al atoms (large gray spheres), O atoms (small gray spheres), C atom (black sphere), H atoms (white spheres), and isosurfaces (white).

have the drawback of not including much of the accidental vdW contribution sometimes seen with ofter functionals, such as LDA with graphene sheets [27]. Thus the inclusion of vdW could significantly change the adsorption energies, especially for the larger molecules like benzene and phenol where they otherwise adsorbed very weakly or not at all. However, for the smaller molecules that were strongly covalently bound to the surface, such as carbonic acid on the alumina surface, the vdW contribution is expected to be insignificant.

Moreover, these results allow us to proceed in producing a simplified potential function for the interaction between BPA-PC and oxidized Al(111) surfaces as well as BPA-PC and alumina. A schematical figure of a BPA-PC monomer can be seen in Fig. 15. In order to provide reliable surface interaction energies it is however necessary to take into account the effect of the nearest neighbor components. This can be done, e.g. as described in Ref. [28], such that our current results form the first step in an iterative procedure. An interesting topic for further study is whether the strong binding of the carbonic acid plays a relevant role when taking the neighboring molecules of the BPA-PC monomer into account, as in that case the passivating hydrogens have been replaced with bonds to the carbon atoms in neighboring benzene molecules. Also, when the entire chain is present, the conformations of the chain itself limits the configurations in which the carbonic acid can come into contact with the surface. However, for building practical materials from these substances the pure surface interaction is not necessarily enough because of the high strains due to the differences in the thermal expansion coefficients of the metal and the polymer, and one would need e.g. mechanical adhesion due to pores

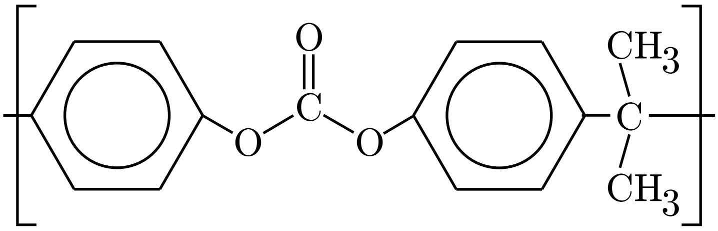

Figure 15. A monomer of the bisphenol-A-polycarbonate molecule. The components from the left are a benzene ring, carbonic acid, another benzene ring, and finally propane.

in the surface, or adhesion promoters such as glue on the surface. In general it seems that the details of the surface chemistry do matter a great deal, e.g. for BPA-PC on Si(001) surfaces hydrogen passivation does completely change the picture [6].

Acknowledgments

The authors wish to thank Professor Risto Nieminen at the Helsinki University of Technology (TKK), Dr. Karen Johnston at the Max Planck Institute for Polymer Science, and our experimental collaborators led by Professor Jyrki Vuorinen at the Tampere University of Technology. This work has been supported by the Finnish Funding Agency for Technology and Innovation (Tekes) through the HYPRIS project, and by the Academy of Finland through its Computational Nanoscience (COMP) Center of Excellence program. We also acknowledge the computer resources provided by the Finnish IT Center for Science (CSC).

[1] P. V. Straznicky, J. F. Laliberté, C. Poon, and A. Fahr. Applications of fiber-metal laminates. *Polymer Composites*, 21:558–567, Apr 2004.

[2] R. Duschek, F. Mittendorfer, R. I. R. Blyth, F. P. Netzer, J. Hafner, and M. G. Ramsey. The adsorption of aromatics on sp-metals: benzene on Al(111). *Chemical Physics Letters*, 318:43–48, 2000.

[3] Svetla D. Chakarova-Käck, Øyvind Borck, Elsebeth Schröder, and Bengt I. Lundqvist. Adsorption of phenol on graphite(0001) and α-Al_2O_3(0001): Nature of van der Waals bonds from first-principles calculations. *Physical Review B*, 74:155402, October 2006.

[4] Chunming Su and Donald L. Suarez. In sity infrared speciation of adsorbed carbonate on aluminum and iron oxides. *Clays and Clay Minerals*, 45(6):814–825, 1997.

[5] C. Alliot, L. Bion, F. Mercier, and P. Toulhoat. Sorption of aqueous carbonic, acetic, and oxalic acids onto α-alumina. *Journal of Colloid and Interface Science*, 287(2):444–451, July 2005.

[6] Karen Johnston and Risto M. Nieminen. Polymer adhesion: First-principles calculations of the adsorption of organic molecules onto Si surfaces. *Physical Review B*, 76:085402, 2007.

[7] Georg Kresse and J. Hafner. Ab initio molecular dynamics for liquid metals. *Physical Review B*, 47(1):558–561, January 1993.

[8] Georg Kresse and Jürgen Furthmüller. Efficiency of ab-initio total energy calculations for metals and semiconductors using a plane-wave basis set. *Computational Materials Science*, 6:15–50, July 1996.

[9] Georg Kresse and Jürgen Furthmüller. Efficient iterative schemes for ab initio total-energy calculations using a plane-wave basis set. *Physical Review B*, 54(16):11169–11186, October 1996.

[10] Björk Hammer, L.B. Hansen, and J.K. Nørskov. Improved adsorption energetics within density functional theory using revised Perdew-Burke-Ernzerhof functionals. *Physical Review B*, 59:7413–7421, Mar 1999.

[11] John P. Perdew, Kieron Burke, and Matthias Ernzerhof. Generalized gradient approximation made simple. *Physical Review Letters*, 77:3865, 1996.

[12] P. E. Blöchl. Projector augmented-wave method. *Physical Review B*, 50(24):17953, 1994.

[13] G. Kresse and D. Joubert. From ultrasoft pesudopotentials to the projector augmented-wave method. *Physical Review B*, 59(3):1758–1775, Jan 1999.

[14] T. J. Godin and John P. Lafemina. Atomic and electronic structure of the corundum (α-alumina) (0001) surface. *Physical Review B*, 49(11):7691, March 1994.

[15] Hendrik J. Monkhorst and James D. Pack. Special points for Brilliouin-zone integrations. *Physical Review B*, 13(12):5188, 1976.

[16] James D. Pack and Hendrik J. Monkhorst. Special points for Brillouin-zone integrations - a reply. *Physical Review B*, 16(4):1748, August 1977.

[17] M. Methfessel and A. T. Paxton. High-precision sampling for brillouin-zone integration in metals. *Physical Review B*, 40(6):3616–3621, August 1989.

[18] David R. Lide, editor. *CRC Handbook of Chemistry and Physics*. CRC Press, 86th edition, 2005.

[19] John P. Perdew, J.A. Chevary, S.H. Vosko, K. A. Jackson, M. R. Pederson, D.J. Singh, and C. Fiolhais. Atoms, molecules, solids, and surfaces: Applications of the generalized gradient approximation for exchange and correlation. *Physical Review B*, 46(11):6671, 1992.

[20] Ann E. Mattsson, Rickard Armiento, Peter A. Schultz, and Thomas R. Mattsson. Nonequivalence of the generalized gradient approximations PBE and PW91. *Physical Review B*, 73:195123, 2006.

[21] Y. Yourdshahayan, B. Razaznejad, and B. I. Lundqvist. Adiabatic potential-energy surfaces for oxygen on Al(111). *Physical Review B*, 65:075416, 2002.

[22] A. Kiejna and B. I. Lundqvist. First-principles study of surface and subsurface O structures at Al(111). *Physical Review B*, 63:085405, 2001. (64) 049901(E).

[23] A. Kiejna and B. I. Lundqvist. Stability of oxygen adsorption sites and ultrathin aluminium oxide films on Al(111). *Surface Science*, 504:1–10, 2002.

[24] Jr. J. N. Russel, A. Leming, and R. E. Morris. Phenol decomposition on Al(111). *Surface Science*, 399:239–247, 1998.

[25] M. Dion, H. Rydberg, E. Schröder, D. C. Langreth, and B. I. Lundqvist. Van der Waals density functional for general geometries. *Physical Review Letters*, 92:246401, June 2004.

[26] M. Dion, H. Rydberg, E. Schröder, D. C. Langreth, and B. I. Lundqvist. Erratum: Van der Waals density functional for general geometries [Phys. Rev. Lett. 92, 246401 (2004)]. *Physical Review Letters*, 95:109902, September 2005.

[27] Masayuki Hasegawa and Kazume Nishidate. Semiempirical approach to the energetics of interlayer binding in graphite. *Physical Review B*, 70(20):205431+, November 2004.

[28] Pim Schravendijk, Luca M. Ghiringhelli, Luigi Delle Site, and Nico F.A. van der Vegt. Interaction of hydrated amino acids with metal surfaces: A multiscale modeling description. *Journal of Physical Chemistry C*, 111:2631–2642, 2007.